

Determining the soil hydraulic conductivity by means of a field scale internal drainage

Gerardo Severino*, Alessandro Santini, Angelo Sommella

Department of Agricultural Engineering and Agronomy, University of Naples 'Federico II', Via Università 100, Portici (Naples) 80055, Italy

Received 16 April 2002; revised 19 November 2002; accepted 22 November 2002

Abstract

Spatial variations of water content in large extents soils (vadose zone) are highly affected by the natural heterogeneity of the porous medium. This implies that the magnitude of the hydraulic properties, especially the conductivity, varies in an irregular manner with scale. Determining mean values of hydraulic properties will not suffice to accurately quantify water flow in the vadose zone. At field scale proper field measurements have to be carried out, similar to standard laboratory methods that also characterize the spatial variability of the hydraulic properties. Toward this aim an internal drainage test has been conducted at Ponticelli site near Naples (Italy) where water content and pressure head were monitored at 50 locations of a $2 \times 50 \text{ m}^2$ plot.

The present paper illustrates a method to quantify the mean value and the spatial variability of the hydraulic parameters needed to calibrate the soil conductivity curve at field scale (hereafter defined as *field scale hydraulic conductivity*). A stochastic model that regards the hydraulic parameters as random space functions (RSFs) is derived by adopting the stream tube approach of Dagan and Bresler (1979). Owing to the randomness of the hydraulic parameters, even the water content θ will be a RSF whose mean value (hereafter termed *field scale water content*) is obtained as an ensemble average over all the realizations of a local analytical solution of Richards' equation. It is shown that the most frequent data collection should be carried out in the initial stage of the internal drainage experiment, when the most significant changes in water content occur.

The model parameters are obtained by a standard least square optimization procedure using water content data at a certain depth ($z = 30 \text{ cm}$) for several times ($t = 5, 24, 48, 96, 144, 216, 312, 408, 576, 744, 912 \text{ h}$). The reliability of the proposed method is then evaluated by comparing the predicted water content with observations at different depths ($z = 45, 60, 75, \text{ and } 90 \text{ cm}$). The calibration procedure is further verified by comparing the cumulative distribution of measured water content at different times with corresponding distribution obtained from the calibrated model.

© 2003 Elsevier Science B.V. All rights reserved.

Keywords: Heterogeneity; Hydraulic conductivity; Internal drainage; Stochastic modelling

1. Introduction

Water flow in the vadose zone is an important problem with applications to groundwater recharge,

irrigation efficiency, and contaminant transport. The hydraulic properties needed to model water flow in the vadose zone are considerably more difficult to obtain. Owing to the enormous field scale variations (e.g. Russo and Bouton, 1992) of the hydraulic conductivity, characterizing its spatial distribution requires many measurements, is time consuming and involves great expense.

* Corresponding author. Tel.: +39-081-2539426; fax: +39-081-2539412.

E-mail address: severino@unina.it (G. Severino).

Consequently, such an intensive sampling effort is practically impossible.

In the last decades, stochastic modelling of spatial variations of soil hydraulic conductivity has been extensively studied by numerous authors (e.g. Yeh et al., 1985a,b; Mantoglou and Gelhar, 1987; Russo and Bouton, 1992; Comegna and Vitale, 1996). The field scale conductivity is estimated as the average over small scales by regarding the local conductivity as a stochastic field. For example, Yeh et al. (1985a,b) determined the mean conductivity curve for steady flows, and similar expressions have also been derived by Green and Freyberg (1995). Mantoglou and Gelhar (1987) used a 3D stochastic approach to evaluate the field scale conductivity under transient conditions; Yeh (1989) determined the hydraulic conductivity by conceptualizing the heterogeneous formation as an equivalent homogeneous medium that will convey the same water flux as the heterogeneous one under the same boundary conditions. Several other publications have addressed the spatial variability of hydraulic conductivity for a vadose zone (e.g. Yeh and Harvey, 1990; Polmann et al., 1991; Russo and Bouton, 1992). Not disregard, in the theory of groundwater flow the same topic has been recently received a big contribute by Indelman (1996, 2001a,b).

The field scale hydraulic conductivity is usually obtained from a large number of soil samples (e.g. Wierenga et al., 1991; Russo and Bouton, 1992). However, it would be much easier especially from the logistic point of view to acquire a time series of water contents rather than to measure the hydraulic conductivity of a large number of cores. In addition, for well known and widely studied hydrological processes like internal drainage (e.g. Hillel, 1998), very simple models are available that enable to identify the field scale hydraulic conductivity. Past work has therefore often focused on the analysis of time series of water content and pressure head during an internal drainage process to determine the unsaturated hydraulic conductivity (e.g. Libardi et al., 1980; Comegna and Basile, 1994). The method of internal drainage provides estimations of the hydraulic conductivity curve using regression of water content data. This method is based on data from individual locations and therefore can give quite variable results because of soil heterogeneity. In order to account for the soil heterogeneity across the field, Romano (1993) has

proposed an inverse geostatistical methodology to characterize the 'spatial structure' of the hydraulic conductivity, while Cahill et al. (1999) have combined the Kalman filter concept and relationships between semivariograms and spatial covariance to identify the field scale hydraulic conductivity.

The present paper aims to derive the field scale hydraulic conductivity from temporal measurements of water content during an internal drainage experiment. The starting point of the analysis is a local analytical solution for water flow, which is subsequently extended to the field scale using the 'column model' concept proposed by Dagan and Bresler (1979). Model parameters are determined by minimizing the mean square deviation between spatial averaged and field scale water content. The reliability of the calibration procedure is then analyzed to verify the capability of the model to independently reproduce water contents across the field.

2. The unsaturated flow model

Methods to determine the hydraulic conductivity based on drainage processes have been widely applied to homogeneous soils in the laboratory using Richards' equation (for a comprehensive exposition, see Romano and Santini, 1999). For large scales, such methods remain valid, but one has to account for the natural heterogeneity, as well. In the past, very few attempts have been made to include the heterogeneity in the calibration procedures and, in any case, they were limited to very simple heterogeneity structures like perfect layering (e.g. Hillel et al., 1972). Unfortunately, the natural soil heterogeneity is more complex.

In order to derive a simple model for water flow at the field scale, we consider the concept of a bundle of columns proposed by Dagan and Bresler (1979). Flow at the column scale is represented by a simple model whose parameters are constant, and flow in each column is independent from adjacent column (i.e. no transversal flow is considered). Area-averaged water content and flux (i.e. the field scale water content and flux) are generated by assuming that the parameters of each column are random variables. The field-scale water content and flux are calculated as an ensemble average over all the realizations of the hydraulic parameters. This implies that, at the field scale, water

content and flux will show much larger variations because of soil heterogeneity. Furthermore, the stream tube model of Dagan and Bresler (1979) assumes that the soil is vertically homogeneous being the heterogeneity only in the horizontal plane (this hypothesis has been relaxed by Indelman et al. (1993)). Such a heterogeneity conceptualization has been used by Indelman et al. (1998) and Lessoff et al. (2003) to study water flow and solute transport for shallow depths (i.e. small compared to the horizontal scale).

To solve flow at the column scale, we assume piston flow with θ (the water content) constant between the soil surface and the water front depth $z_f = z_f(t)$. Although this approximation leads to θ -profiles that significantly differ from those according to Richards' equation (Richards, 1931), the results are sufficiently accurate for the field scale water content (see Fig. 1) due to the averaging effect over all the columns. The 1D governing equations for gravitational flow (unit gradient flow) conditions are written as

$$q = K(\theta), \quad \frac{\partial \theta}{\partial t} + \frac{\partial q}{\partial z} = 0 \quad (1)$$

(the vertical coordinate z is pointing downwards). The solution of Eq. (1) is achieved by adopting the Brooks and Corey (1964) model for the conductivity

$$K(\theta) = K_s \left(\frac{\theta - \theta_r}{\theta_s - \theta_r} \right)^{1/\beta}, \quad (2)$$

where θ_r and θ_s are the residual and saturated water content, respectively, β is a pore-distribution dependent parameter, and K_s is the saturated hydraulic conductivity. Details of the derivation are given in Appendix A. The final results are

$$\theta(z, t; K_s) = \theta_r + (\theta_s - \theta_r) \Theta^{-\beta}(t) H[z_f(t) - z], \quad (3)$$

$$q(z, t; K_s) = K_s \Theta^{-1}(t) H[z_f(t) - z]$$

$$\Theta(t) = 1 + \frac{K_s t}{\beta W}, \quad z_f(t) = \frac{W}{\theta_s - \theta_r} \Theta^\beta(t). \quad (4)$$

In Eq. (4), W represents the total volume of applied water per unit area, which determines saturation conditions up to $z_f = W/(\theta_s - \theta_r)$ (see Appendix A for details).

As also shown by Indelman et al. (1998), the drainage front $z_f = z_f(t)$, is unbounded with the time

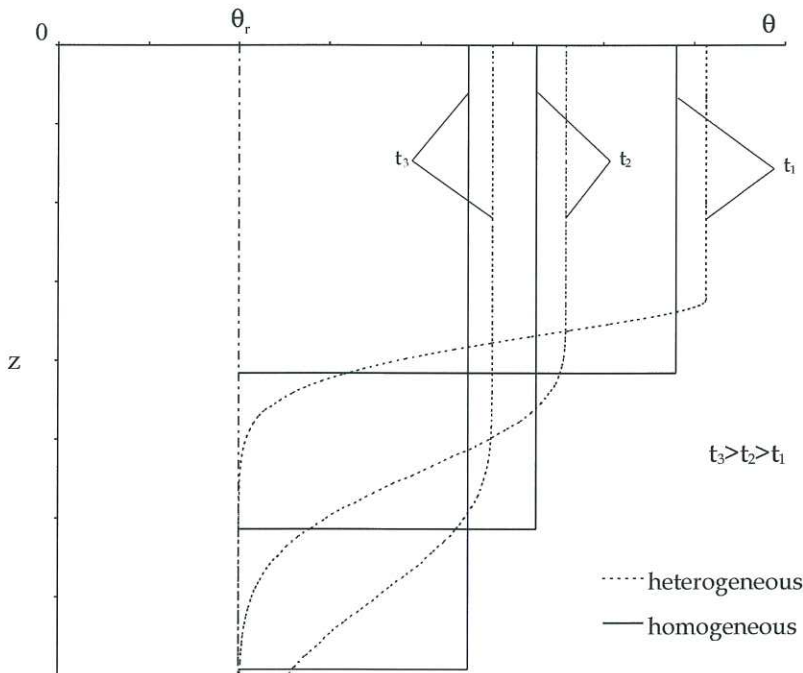


Fig. 1. Definition sketch of local (continuous line) and field scale (dashed line) water content profiles.

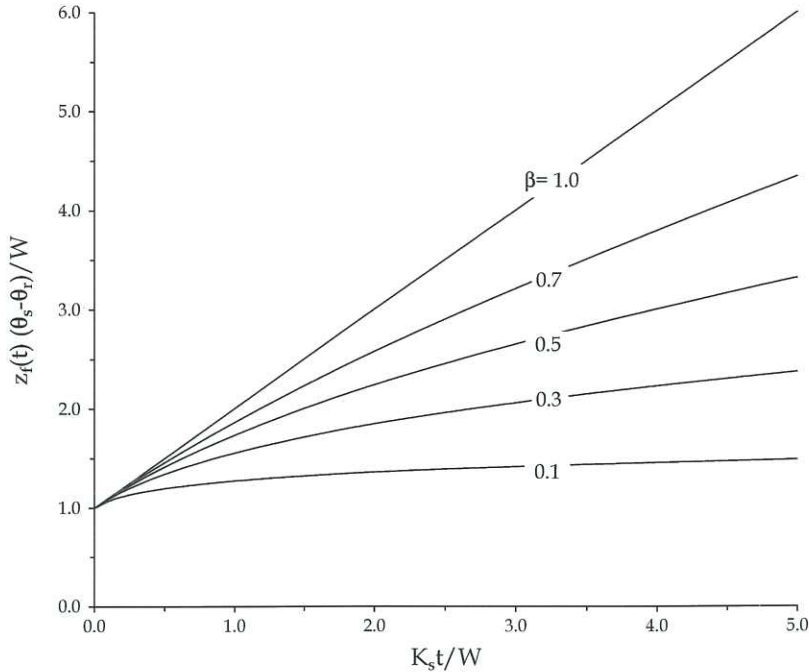


Fig. 2. Water front $z_r(t)(\theta_s - \theta_r)/W$ versus the dimensionless time tK_s/W for several values of β .

(Fig. 2). On the other hand, the water content θ and flux q are decreasing with time (Fig. 3a and b). In particular, the water content (θ) is the sum of the residual water content (θ_r) and a function approaching zero for $t \rightarrow \infty$. Both the saturation $S = (\theta - \theta_r)/(\theta_s - \theta_r)$ and flux (see Fig. 3a and b) range from their maximum values (at $t = 0$) and 0 obtained for $t \rightarrow \infty$. The rate of decrease is governed by the value of β . Averaging Eq. (3) over all the realizations of the random variables, $K_s, \beta, \theta_s, \theta_r$ yields the desired field scale water content and flux

$$\langle \theta(z, t) \rangle = \int \dots \int \theta(z, t; K_s, \beta, \theta_s, \theta_r) f(K_s, \beta, \theta_s, \theta_r) \times dK_s d\beta d\theta_s d\theta_r \quad (5)$$

$$\langle q(z, t) \rangle = \int \dots \int q(z, t; K_s, \beta, \theta_s, \theta_r) f(K_s, \beta, \theta_s, \theta_r) \times dK_s d\beta d\theta_s d\theta_r \quad (6)$$

where $f = f(K_s, \beta, \theta_s, \theta_r)$ is the joint probability distribution of $K_s, \beta, \theta_s, \theta_r$. Calculating Eqs. (5) and (6) requires a multiple integration of the solutions for the column scale given by Eq. (3).

In numerous field experiments (e.g. Bresler and Dagan, 1981; Butters et al., 1989; Comegna and

Basile, 1992; Indelman et al., 1998), the variability of most of the hydraulic parameters (i.e. $\beta, \theta_s, \theta_r$) was found to be small as compared with that of K_s . It is therefore reasonable to regard these parameters constant and equal to their mean values, i.e. $\beta \approx \langle \beta \rangle, \theta_s \approx \langle \theta_s \rangle,$ and $\theta_r \approx \langle \theta_r \rangle$. Thus, the saturated conductivity K_s remains the only random space function (RSF) that we assume log-normally distributed (in line with many field findings, e.g. Russo and Bouton, 1992)

$$f(K_s; \langle K_s \rangle, \xi) = \frac{1}{\sqrt{2\pi \ln(1 + \xi^2)} K_s} \times \exp \left\{ - \frac{\left[\ln \left(\frac{K_s}{\langle K_s \rangle} \sqrt{1 + \xi^2} \right) \right]^2}{2 \ln(1 + \xi^2)} \right\} \quad (7)$$

with given mean ($\langle K_s \rangle$) and coefficient of variation (ξ).

The decrease of the mean water content with time is shown in Fig. 4, which depicts the mean saturation $\langle S \rangle = (\langle \theta \rangle - \theta_r)/(\theta_s - \theta_r)$ versus the dimensionless depth $z' = z(\theta_s - \theta_r)/W$ for $t' = t\langle K_s \rangle/W = 0.05; 0.25; 0.5; 1; 3; 10; 100$ using $\xi = 1$ and $\beta = 0.25$.

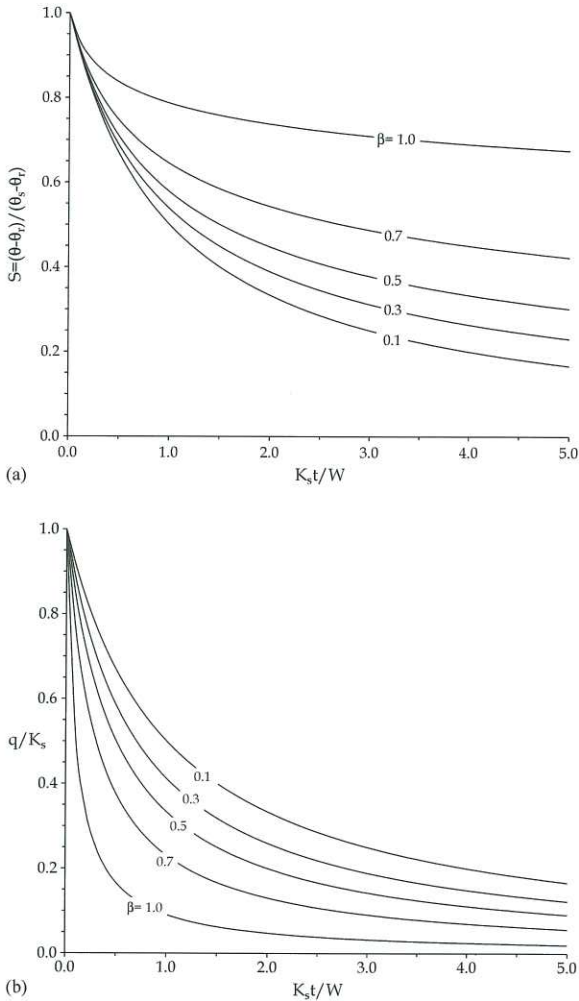


Fig. 3. Saturation (a) and flux (b) versus time for several values of β .

The mean saturation profile is quite uniform for $z' \leq 1$, while the impact of heterogeneity is mainly relevant across the drainage front. At early times, $\langle S \rangle$ decreases very fast with about 30% ($0 \leq t' \leq 1$), whereas for larger times reductions are much lesser pronounced. Thus, in order to determine a wide range of water content data, it is important to record water content during the early stages of the internal drainage experiments.

In many field applications it is customary to use the mean value of K_s for the conductivity instead of using the more complex concept of field hydraulic conductivity. To assess the merits of this practice, we have introduced the parameter α which is the ratio between

K_{field} (given by Eq. (6)) and K_h (calculated from the second of Eq. (3) by assuming K_s is equal everywhere to its mean value)

$$\alpha = \frac{K_{\text{field}}}{K_h}. \quad (8)$$

The parameter α is plotted versus the dimensionless time $t' = t(K_s)/W$ in Fig. 5 and for several ξ . The main result is that α attains the lowest value (say α_{min}) for $t' < 1$ suggesting that the impact of heterogeneity is mainly felt at the early times. Furthermore, the differences between K_{field} and K_h are very significant for $\xi \geq 2$ resulting in $0.5 \leq \alpha_{\text{min}} \leq 0.70$. In all cases K_h represents an overestimation of K_{field} . The impact of heterogeneity can be completely neglected in the asymptotic regime, i.e. $\alpha \rightarrow 1$ for $t' \rightarrow \infty$. The value for ξ determines how soon the asymptotic regime is reached. However, using K_h although more convenient, does not provide any information about the spatial variability of the hydraulic conductivity.

Summarizing the results of this section, first an analytical solution for local gravity-driven water drainage was presented. Then, by using the column model of Dagan and Bresler (1979), we derived the field scale flux $\langle q \rangle$ and water content $\langle \theta \rangle$. These quantities generally are expressed as multiple integrals (Eqs. (5) and (6)) and involve the knowledge of the joint probability distribution f of the all spatially variable parameters. The calibration of the field scale hydraulic conductivity is obtained by optimizing Eq. (5) to measurements which should be taken most frequently at the early stage. In Section 3 we shall apply the proposed procedure to an actual experimental data.

3. Application

The field scale drainage model derived in Section 2 can be used to determine the corresponding field scale hydraulic conductivity. We shall apply the model to a field drainage experiment during which water content profiles and pressure head were measured at 50 locations for several times. We will first briefly summarize the experiment, then describe the model calibration and finally a comparison with independent data is shown.

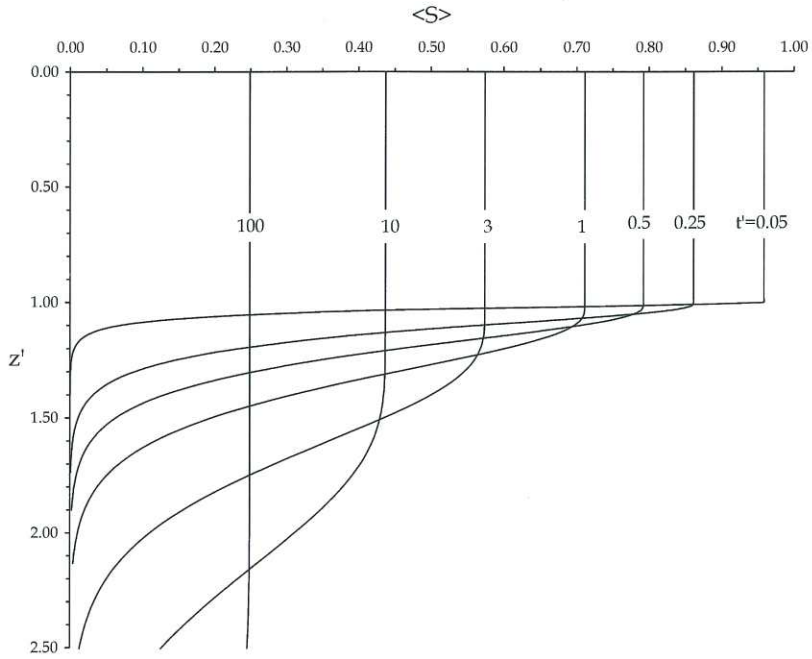


Fig. 4. Mean saturation $\langle S \rangle = (\langle \theta \rangle - \theta_r) / (\theta_s - \theta_r)$ along the dimensionless depth $z' = z(\theta_s - \theta_r) / W$ for $t' = t(K_s) / W = 0.05; 0.25; 0.5; 1; 3; 10; 100$. Parameter values: $\beta^{-1} = 4$ and $\xi = 1$.

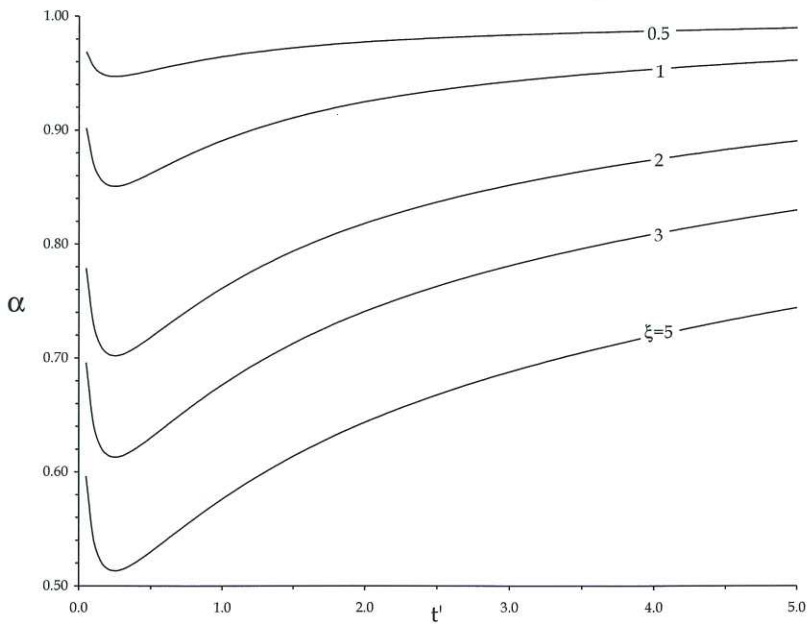


Fig. 5. Characteristic parameter α , ratio between the field scale hydraulic conductivity and the mean conductivity, versus the dimensionless time $t' = t(K_s) / W$ for several values of the coefficient of variation ξ . Parameter values: $\beta^{-1} = 4$ and $z' = z(\theta_s - \theta_r) / W = 0.2$.

3.1. The field experiment

The experiment was conducted on a sandy soil located at the Ponticelli site near Naples (Italy). The soil, with no layering, is classifiable as an Andosol whose bulk density was equal to 1.2 g/cm^3 . At the center of the field where the trial was carried out, a $2 \times 50 \text{ m}^2$ plot was prepared by constructing a 0.25 m high boundary ridge. This ridge was used to control and allow measurement of the total applied water volume needed to saturate the soil (at least in the most upper part of the soil profile were the instruments were located). At the center of the plot, 50 access 1.5 m tubes were inserted at constant intervals of 1 m to measure water contents at $z = 30, 45, 60, 75$ and 90 cm depth with a neutron probe (see Fig. 6). In order to reduce instrument error, which essentially depends on fluctuations in counting rate due to random variation in the fast neutron-emission from the source, three readings per depth were averaged. The adopted counting time was 1 min. Readings were then divided by the standard reading to obtain a count-ratio which was referred to the field calibration curve to infer water content (Ciollaro and Comegna, 1989). In this way, water contents indirectly determined by neutron probe were very little affected by instrumental as well as experimental uncertainties (see Comegna and Basile, 1992). Along a parallel transect, at 0.50 m from the tube axes, mercury-water manometer-type tensiometers were installed at a depth of 0.30 m to register the pressure head (see Fig. 6). The ceramic

tensiometer cups were made according to the following characteristics: (i) the bubbling pressure was greater than 0.5 bar, (ii) the cup conductance was greater than $0.0111 \text{ cm}^{-3} \text{ s}^{-1} \text{ bar}^{-1}$ of pressure difference across the wall, and (iii) the gauge sensitivity was equal to 1 bar/cm^3 . At some of the 50 locations, tensiometers were also installed at $z = 45, 60, 75$ and 90 cm to determine the pressure head distribution during the drainage (Comegna and Basile, 1992). Of course, it would have been worthwhile to have such a massive instrumentation in each sampling location to properly record the pressure head, but this was impossible because of logistic limitations. Nevertheless, since the flow was practically vertical up to $t = 912 \text{ h}$ (Ciollaro et al., 1989) pressure head data were not essential in order to determine the field scale hydraulic conductivity.

For purposes of the trial, the plot was ponded by applying water in excess of the infiltration rate, while an overflow pipe guaranteed a constant water depth of 0.15 m. The time required to establish steady-state conditions for the first 1 m, was about a week. When infiltration was halted, the plot surface was covered with a plastic sheet to avoid evaporation and rainfall. Measurements were carried out at several times (5, 24, 48, 96, 144, 216, 312, 408, 576, 744, 912 h) from the start of the internal drainage. The water content θ and the head Ψ were measured at the same times, thereby making it easier to determine the retention curve. Monitoring was interrupted 42 days after the end of infiltration when the drainage was evolving too slowly

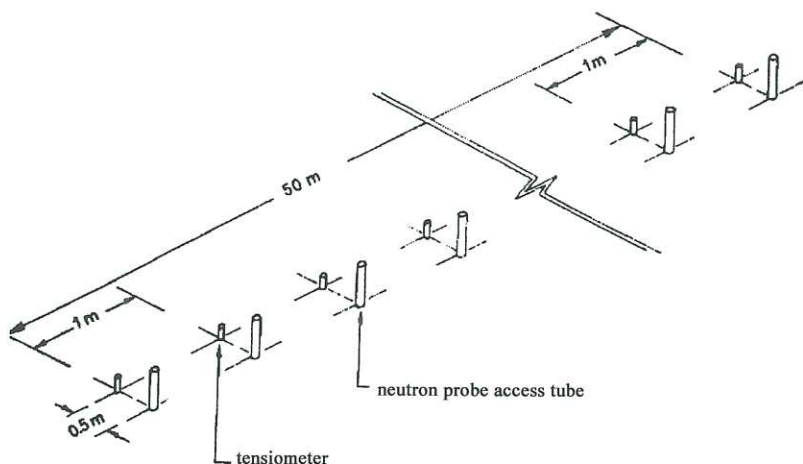


Fig. 6. Spatial arrangement of the experimental plot at Ponticelli site near Naples (Italy).

Table 1
Mean value and coefficient of variation of water content θ and pressure head Ψ for $z = 30$ cm at the sampling times

t (h)	$\bar{\theta}$ (cm ³ /cm ³)	$-\bar{\Psi}$ (cm)	CV(θ)	CV($-\Psi$)
5	0.381	50.664	0.206	0.068
24	0.340	83.300	0.126	0.077
48	0.319	101.719	0.098	0.081
96	0.299	128.795	0.106	0.082
144	0.287	147.326	0.111	0.081
216	0.274	166.476	0.106	0.082
312	0.265	184.508	0.113	0.081
408	0.257	202.865	0.102	0.085
576	0.247	225.638	0.103	0.087

to collect meaningful data. Upon completion of the experiment, at every measuring point, undisturbed soil samples were taken to determine the texture which resulted as follows: 80% sand, 12% silt, and 8% clay. For purposes of illustration, in Table 1 we have reported for each time of measurement the main statistical parameters (i.e. mean and coefficient of variation) of water content and pressure head at $z = 30$ cm.

3.2. The model calibration

The field scale water content $\langle\theta\rangle$ depends upon various parameters. Ideally, the parameters should be determined using a laboratory methodology which relies on soil samples (e.g. Romano and Santini, 1999). However, this approach is impracticable at field scale since: (i) data collection would require an enormous number of samples, and (ii) the laboratory procedure based on small soil cores may result error prone in the sense that samples are not representative enough in the context of the REV concept (Bear, 1972). Thus, we have gathered all the parameters from in situ measurements.

It is well known (e.g. Bresler and Dagan, 1981; Butters et al., 1989; Russo et al., 1997; Indelman et al., 1998) that some parameters like β , θ_s , and θ_r exhibit a lesser variability than others and this was also found for the Ponticelli experiment. As pointed out by Romano (1993), the spatial distribution of β , θ_s , and θ_r showed very small variations along the transect and only slight differences were observed in the measurements carried out at the end of the drainage (this was presumably due to the lack of precision of instruments

at the low water contents). Because of these very small fluctuations, we will attribute all the heterogeneity to the saturated conductivity K_s , which will be described by a univariate log-normal distribution (7) to calculate the field scale water content $\langle\theta\rangle$ and flux $\langle q\rangle$ from Eqs. (5) and (6). Because the specific volume W was uniformly applied (see Section 3.3 for details), we can consider it constant and equal to 91.7 cm (Comegna and Basile, 1992). The water content at saturation (θ_s) was estimated from measurements carried out at the beginning of the experiment when all the sampling points had reached saturation leading to $\theta_s = 0.409$ cm³/cm³ (CV(θ_s) = 0.07). Information from previous measurements in the same transect (Comegna and Basile, 1992) suggested that $\theta_r = 0.15$ cm³/cm³.

The remaining parameters were estimated by an optimization procedure. The most extensive measurements were water content data at $i = 50$ locations, along $j = 5$ depths, and for $k = 11$ times. The spatially averaged water content $\bar{\theta}$ for a particular time and depth was determined by averaging data at different locations of the transect

$$\bar{\theta}(z_j, t_k) = \frac{1}{50} \sum_{i=1}^{50} \theta_i(z_j, t_k). \quad (9)$$

At this point it is worth to recall that while the model refers to all possible realizations of the medium (quantities (5) and (6) are derived in the sense of ensemble averages), the field data were obtained from spatial averages. The identification of ensemble average from the spatial one, i.e.

$$\bar{\theta}(z_j, t_k) \approx \langle\theta(z_j, t_k)\rangle \quad (10)$$

assumes ergodicity (e.g. Dagan, 1989). The pragmatic approach adopted here, in line with that of the statistical continuum theories (e.g. Beran, 1968), is to presume that ergodicity holds, at the least up to the second order level.

We carried out a simple least-squares optimization procedure using a Levenberg–Marquardt algorithm (e.g. Gill et al., 1981) toward defining β , $\langle K_s\rangle$, and ξ by fitting the spatial average of the drainage profile at $z_1 = 30$ cm, i.e. $\bar{\theta}(z_1, t_k)$, against the field scale water content $\langle\theta\rangle$ that is calculated by numerically carrying out the quadrature appearing in Eq. (5). The best optimization was achieved

when: (i) $\langle K_s \rangle = 2.58$ cm/h, (ii) $\xi = 0.524$, and (iii) $\beta^{-1} = 4.24$ ($R^2 = 0.987$). In Section 3.3, we discuss the reliability of the optimized parameters using independent data sets.

3.3. Comparison with independent data

Six different water content profiles corresponding to $t = 5, 24, 48, 96, 144,$ and 312 h, were selected to test the reliability of the calibrated model. We calculated the spatial mean value of water content ($\bar{\theta}$) along the depth by averaging the measurements at the device-depth for a fixed time. These profiles are used for comparative purposes with the simulations carried out by using the optimized field scale hydraulic conductivity as determined in Section 3.2. In Fig. 7 we have depicted $\bar{\theta}$ (symbols) and $\langle \theta \rangle$ (line). Overall, the simulated results describe the data reasonably well. Observe that we limit to consider up to $t \leq 312$ h, as for larger times water was observed practically immobile. For purposes of comparison with experimental data, in Fig. 7 we have shown only the most upper part of the soil where

the water content profile is vertical by virtue of the gravitational regime (of course the water content profile $\langle \theta \rangle$ is not a linear function as it is clearly seen in Fig. 4).

We have already remarked that, due to the randomness of K_s , the water content θ will also be RSF with mean given by Eq. (5) and with variance

$$\sigma_{\theta}^2 = \langle \theta^2 \rangle - \langle \theta \rangle^2. \quad (11)$$

Generally, the first two moments (5) and (11) are not sufficient to completely characterize the spatial distribution of the water-content. However, for the Ponticelli experiment, it was observed that the water content is log-normally distributed (Comegna and Vitale, 1996). This allows us to derive the cumulative distribution of θ and compare it with the distribution estimated from measurements. In Fig. 8 we have depicted (symbols) the estimated cumulative function $F(\theta)$ versus $\ln \theta$ at several times and a fixed depth ($z = 45$ cm). At a first glance, it is clearly seen that the log-normal model describes the behavior of the water content with time fairly well. This suggests that to characterize the water content, the first two moments

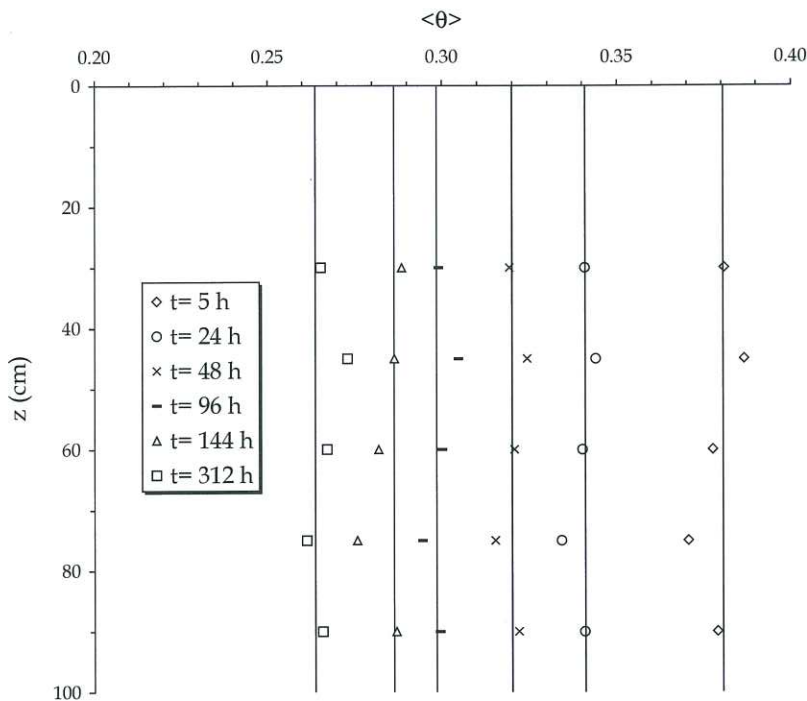


Fig. 7. Mean water content profile as calculated from data (symbols) and the model (line) at selected sampling times. Parameter values: $\theta_s = 0.409$, $\theta_r = 0.15$, $\beta^{-1} = 4.24$, $\xi = 0.524$, $\langle K_s \rangle = 2.58$ cm/h.

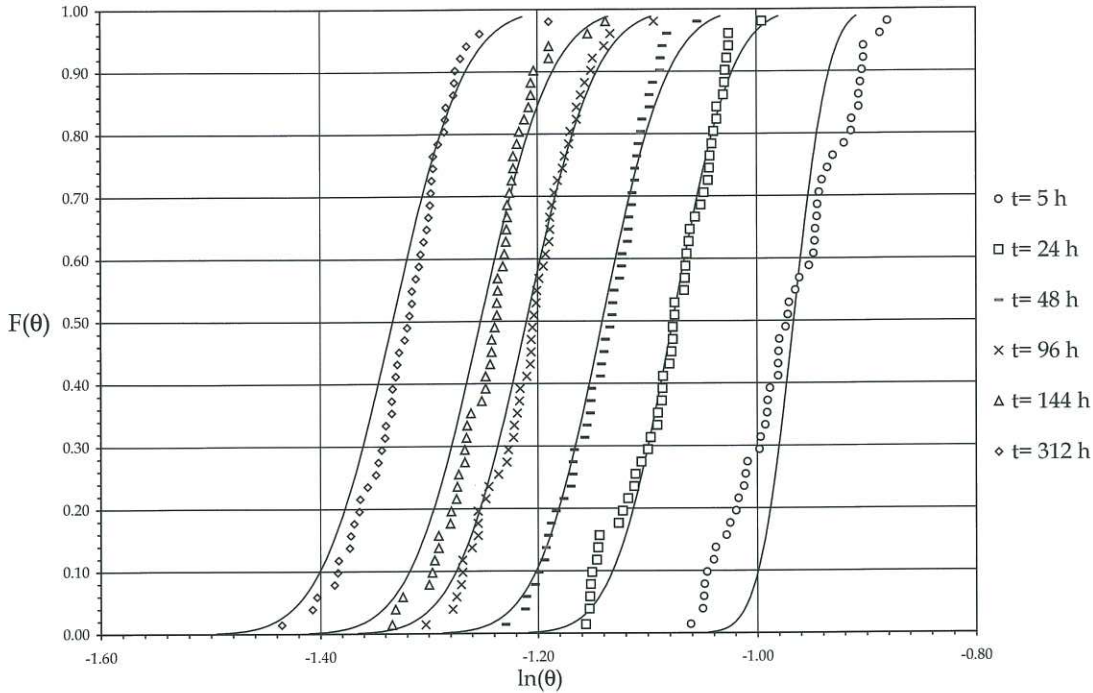


Fig. 8. Cumulative distribution function of $\ln(\theta)$ estimated from data (symbols) and from the model (lines) for few times. Parameter values: $\theta_s = 0.409$, $\theta_r = 0.15$, $\beta^{-1} = 4.24$, $\xi = 0.524$, $\langle K_s \rangle = 2.58$ cm/h.

are sufficient. In Fig. 8 we have also depicted the theoretical distribution (line) as calculated from the optimized parameters. For $t \geq 24$ h, the agreement between the theoretical curves and the experimental data is quite good. For earlier times ($t = 5$ h), there is a discrepancy presumably due to a higher dispersion in experimental data as compared with the model. The likely reason is the time needed to measure water contents for all profiles at the 50 locations of the transect. In fact, each sampling procedure took about 1 h (Comegna and Basile, 1992). Since drainage rapidly evolves during

the early time regime, measurements collected over an interval of roughly 1 h are affected by a higher variability because of logistic limitations of data recording. To facilitate quantitative comparisons, Table 2 reports the estimated and theoretical means, variances, and coefficients of variation of $\zeta = \ln \theta$.

The calibration was conducted by using the drainage profile at $z = 30$ cm, therefore we have evaluated the model by considering drainage profiles at the remaining depths, i.e. $z = 45, 60, 75,$ and 90 cm. It is important to recall that the soil at the beginning of the drainage is fully saturated

Table 2
Mean value, variance, and coefficient of variation of $\zeta = \ln(\theta)$ from observations and modeling at the sampling times

t (h)	$(\bar{\zeta})_{\text{data}}$	$(\bar{\zeta})_{\text{model}}$	$10^2 (\text{VAR}(\zeta))_{\text{data}}$	$10^2 (\text{VAR}(\zeta))_{\text{model}}$	$10^2 (\text{CV}_{\zeta})_{\text{data}}$	$10^2 (\text{CV}_{\zeta})_{\text{model}}$
5	-0.971	-0.960	0.200	0.063	-4.61	-2.62
24	-1.080	-1.078	0.177	0.208	-3.90	-4.23
48	-1.140	-1.142	0.160	0.254	-3.51	-4.41
96	-1.206	-1.215	0.186	0.267	-3.58	-4.25
144	-1.245	-1.258	0.162	0.261	-3.23	-4.06
312	-1.323	-1.335	0.201	0.234	-3.39	-3.62

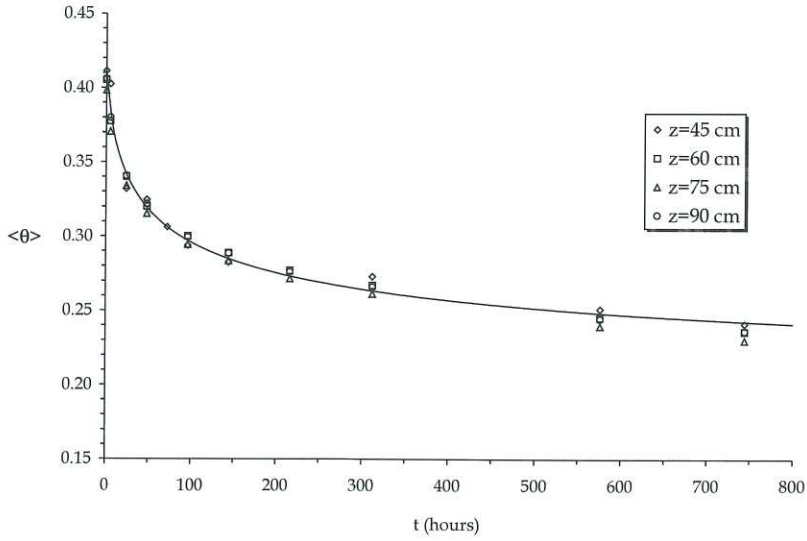


Fig. 9. Drainage curves at $z = 45, 60, 75,$ and 90 cm calculated from the model (line) and data (symbols). Parameter values: $\theta_s = 0.409$, $\theta_r = 0.15$, $\beta^{-1} = 4.24$, $\xi = 0.524$, $\langle K_s \rangle = 2.58$ cm/h.

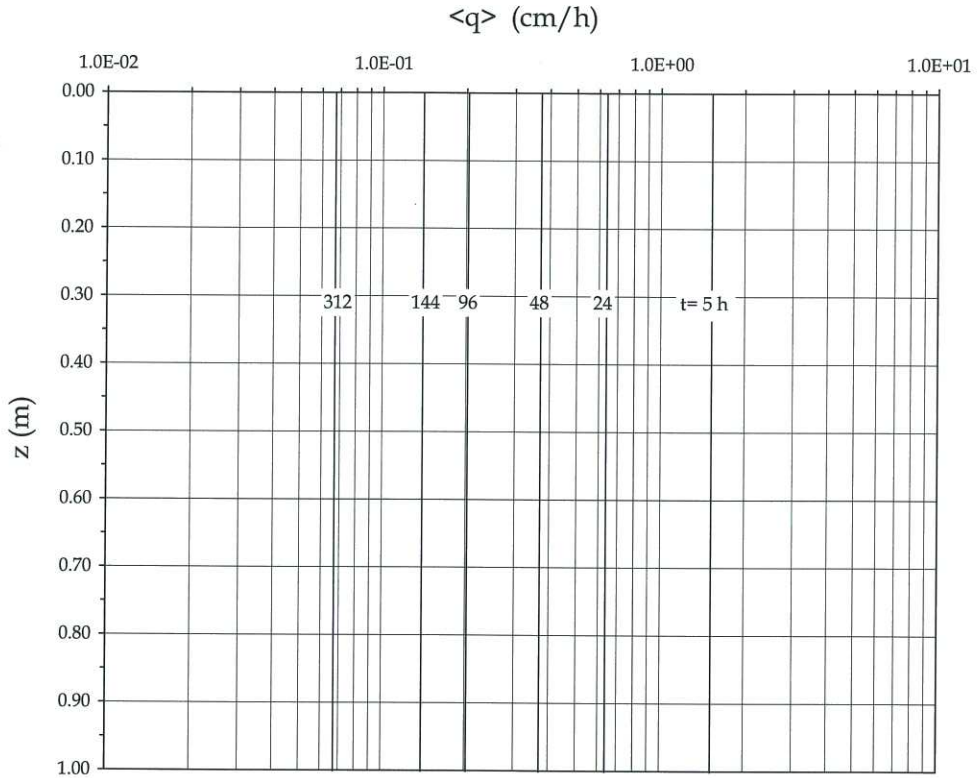


Fig. 10. Estimated field scale flux $\langle q \rangle$ versus depth.

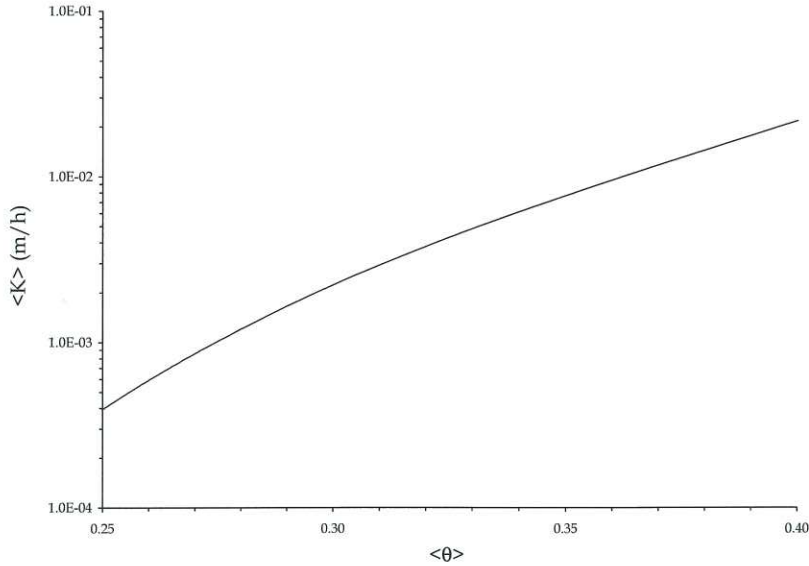


Fig. 11. Field scale hydraulic conductivity curve as estimated from the calibration procedure.

(at least the zone where the data were collected), and that, because of mass conservation coupled with the gravitational flow regime, the amount of water transferred to the lower depths will therefore remain the same. As a result, the drainage profile is almost the same at each depth. This is shown in Fig. 9 in which it is quite evident that the drainage curves (symbols) at the various sampling depths ($z = 45, 60, 75,$ and 90 cm) match the calibrated curve for $z = 30$ cm (line) very well.

From inspection of Figs. 7–9 it is evident that the identified parameters lead to a very satisfactory description of independently observed data. The mean value of the flux, as determined from the calibration at different times is depicted in Fig. 10. As expected from water content pattern (see Fig. 7), the flux decreases very drastically after 24 h and continues to diminish afterwards although with lesser temporal gradients, until it practically halts after 312 h from the beginning of the drainage. This behavior is important for experimental design purposes as it illustrates again that the water content sampling during an internal drainage experiment has to be very frequent during the early stages. For completeness, we have also depicted in Fig. 11 the field scale hydraulic

conductivity $\langle K \rangle$ versus the field scale water content $\langle \theta \rangle$.

4. Summary and conclusions

In the present paper we have determined the field scale soil hydraulic conductivity using data from an internal drainage experiment during which the water content and pressure head were monitored at different depths and times (with zero evapotranspiration at the inlet). These measurements were used to estimate the field scale hydraulic conductivity using an inverse method like the standard laboratory procedure (Romano and Santini, 1999). At laboratory scale the hydraulic parameters are regarded constant, but in our study they are spatially variable because of the natural soil heterogeneity. To simplify the computational effort, we have applied some approximations similar to those used by Indelman et al. (1998) when studying solute transport in the vadose zone under an infiltration/redistribution cycle.

This study consists of two parts. In the first part, we adopt the model of Dagan and Bresler (1979) to obtain a field solution for water flow. This is achieved by regarding the soil as a collection of

homogeneous, vertical columns each with different properties in the horizontal plane. The mean water content and flux are obtained by multiple quadrature of the local solutions weighted by the joint probability distribution of hydraulic parameters. To perform simple computations, we have attributed all the assessed soil heterogeneity to the spatial variation of the saturated hydraulic conductivity K_s , which was modelled as a stationary RSF of horizontal coordinates. Because the field scale drainage evolves very rapidly during the early times, frequent data recording is needed during this stage. The applicability of a simpler approach, i.e. using the mean conductivity without accounting for the more complex field scale hydraulic conductivity, is also discussed.

In the second part, we applied the proposed model to actual data from a drainage experiment. The calibration of the model was done by considering water content measurements at $z = 30$ cm. The availability of independent (in the sense that they were not used in the calibration procedure) data enabled us to conduct a comprehensive reliability analysis of the calibration. The distribution with the depth (at several times) of the water content was quite close to the spatial average. Furthermore, the cumulative distribution function of θ was in close agreement with the one predicted by the model. An appreciable difference was only observed in the very early stage where the experimental data exhibit more dispersion than the predicted curve. This is presumably due to the 1 h time required for data collection. Moreover, the water content profiles at the other sampling depths, i.e. $z = 45, 60, 75,$ and 90 cm showed no significant deviations from the profile at $z = 30$ cm. This suggests, again, the reliability of the calibrated model in reproducing independently measured data.

The results of this study provide a new tool to deal with water flow in heterogeneous soils. It will find application for prediction the fate of chemicals in agricultural soils and groundwater pollution. Of course, this study is not exhaustive and there are many directions toward it can be generalized. For instance, removing the assumption of gravitational flow as well as considering three-dimensional

structure for the hydraulic conductivity represent important topics for future studies.

Acknowledgements

This study was partly supported by the grant 'Giovani ricercatori' Trasporto di soluti in suoli eterogenei: sviluppo e verifica di un modello matematico (D. R. n. 4385, 28/12/2000). Sincere thanks to Feike Leij for his helpful suggestions. We are grateful to two anonymous reviewers for their thoughtful comments.

Appendix A. Solution of water flow

Assuming gravitational regime, Eq. (1) yield

$$\frac{\partial \theta}{\partial t} + \frac{\partial K}{\partial z} = 0. \quad (\text{A1})$$

We consider the flow subsequent to the application at the surface ($z = 0$) of a certain amount W of water, which determines saturated conditions up to a certain depth z_f (i.e. a step distribution). Drainage occurs with zero flux at the surface, i.e. $q(0, t) = 0$. A solution of Eq. (A1) is sought in the following form

$$\theta(z, t) = \theta_r + (\theta_s - \theta_r)S(t)H[z_f(t) - z] \quad (\text{A2})$$

$$q(z, t) = K(\theta)H[z_f(t) - z] \quad (\text{A3})$$

where $S(t)$ is a function to be determined and $z_f(t)$ satisfies the mass conservation and the kinematical law

$$W = (\theta - \theta_r)z_f(t) \quad \frac{dz_f}{dt} = \frac{K(\theta)}{\theta - \theta_r} \quad (\text{A4})$$

(H is the Heaviside step function). Observe that from the mass conservation law, the soil is initially at $\theta = \theta_s$ from $z = 0$ to $z_f(0) = W/(\theta_s - \theta_r)$ whereas $\theta = \theta_r$ below $z_f(0)$. The initial saturated depth was equal to $W/(\theta_s - \theta_r)$ which is in accordance with the recent model for infiltration/redistribution proposed by Indelman et al. (1998). We obtain from the first of Eq. (A4), by using the chain rule of derivation

$$\begin{aligned} \frac{dz_f}{dt} &= \frac{d\theta}{dt} \frac{dz_f}{d\theta} = \frac{d\theta}{dt} \frac{d}{d\theta} \left(\frac{W}{\theta - \theta_r} \right) \\ &= - \frac{W}{(\theta - \theta_r)^2} \frac{d\theta}{dt}. \end{aligned} \quad (\text{A5})$$

Substituting in the second of Eq. (A4) leads to the following initial value problem

$$\frac{d\theta}{dt} = -\frac{(\theta - \theta_r)K(\theta)}{W} \quad \theta(0) = \theta_s. \quad (\text{A6})$$

By virtue of Eq. (2), Eq. (A6) can be written as

$$\frac{d\theta}{dt} = -\Delta(\theta - \theta_r)^{1+(1/\beta)} \quad \theta(0) = \theta_s, \quad (\text{A7})$$

$$\left(\Delta = \frac{K_s}{W} (\theta_s - \theta_r)^{-1/\beta} \right)$$

whose solution is

$$\theta = \theta_r + (\theta_s - \theta_r)\Theta^{-\beta}(t) \quad (S(t) = \Theta^{-\beta}(t)) \quad (\text{A8})$$

$$\Theta(t) = 1 + \frac{K_s t}{\beta W} \quad (\text{A9})$$

while the drainage front is obtained from the first of Eq. (A4) as

$$z_f(t) = \frac{W}{\theta_s - \theta_r} \Theta^\beta(t). \quad (\text{A10})$$

Thus, the specific discharge q results from Eq. (A3) as

$$q(z, t; K_s) = K_s \Theta^{-1}(t) H[z_f(t) - z]. \quad (\text{A11})$$

References

- Bear, J., 1972. Dynamics of Fluids in Porous Media, Dover, New York.
- Beran, M.J., 1968. Statistical Continuum Theories, Wiley Interscience, New York.
- Bresler, E., Dagan, G., 1981. Convective and pore scale dispersive solute transport in unsaturated heterogeneous fields. Water Resources Research 17, 1683–1693.
- Brooks, P.M., Corey, A.T., 1964. Hydraulic properties in porous media. Hydrol. Paper 3, University of Colorado, Fort Collins.
- Butters, G.L., Jury, W.A., Ernst, F.F., 1989. Field scale transport of bromide in unsaturated soil, 1, Experimental methodology and results. Water Resources Research 25, 1575–1581.
- Cahill, A.T., Ungaro, F., Parlange, M.B., Mata, M., Nielsen, D.R., 1999. Combined spatial and Kalman filter estimation of optimal soil hydraulic properties. Water Resources Research 35, 1079–1088.
- Ciollaro, G., Comegna, V., 1989. Methodology for the study of hydraulic properties of soil on a plot scale. Proceedings of the XI International Congress of Agricultural Engineering 1, 471–480.
- Ciollaro, G., Comegna, V., Ruggiero, C., 1989. Comparison of field and laboratory measured soil hydraulic properties of a soil. Irrigazione e Drenaggio 3, 67–72.
- Comegna, V., Basile, A., 1992. Spatial and temporal variability of soil water content. Internal Report, 1–17. in Italian.
- Comegna, V., Basile, A., 1994. Temporal stability and spatial patterns of soil water storage in a cultivated Vesuvian soil. Geoderma 62, 299–310.
- Comegna, V., Vitale, C., 1996. Statistical Analysis of Soil Hydraulic Properties (in Italian), CUSL Edition.
- Dagan, G., 1989. Flow and Transport in Porous Formations, Springer, Berlin.
- Dagan, G., Bresler, E., 1979. Solute dispersion in unsaturated heterogeneous soil at field scale: theory. Soil Science Society of America Journal 43, 461–467.
- Gill, P.E., Murray, W., Wright, M.H., 1981. Practical Optimization, Academic Press, New York.
- Green, T.R., Freyberg, D.L., 1995. State-dependent anisotropy: comparisons of quasi-analytical solutions with stochastic results for steady gravity drainage. Water Resources Research 31, 2201–2212.
- Hillel, D., 1998. Environmental Soil Physics, Academic Press, New York.
- Hillel, D., Krentos, V., Stylianou, Y., 1972. Procedure and test of an internal drainage method for measuring hydraulic characteristics in situ. Soil Science 114, 395–400.
- Indelman, P., 1996. Averaging of unsteady flows in heterogeneous media of stationary conductivity. Journal of Fluid Mechanics 310, 39–60.
- Indelman, P., 2001a. Steady-state source flow in heterogeneous porous media. Transport in Porous Media 1548, 1–23.
- Indelman, P., 2001b. Unsteady source flow in weakly heterogeneous porous media. Computational Geosciences 4, 351–381.
- Indelman, P., Or, D., Rubin, Y., 1993. Stochastic analysis of unsaturated steady state flow through bounded heterogeneous formations. Water Resources Research 29, 1141–1147.
- Indelman, P., Touber-Yasur, I., Yaron, B., Dagan, G., 1998. Stochastic analysis of water flow and pesticides transport in a field experiment. Journal of Contaminant Hydrology 32, 77–97.
- Lessoft, S.C., Indelman, P., Dagan, G., 2002. Solute transport in infiltration–redistribution cycles in heterogeneous soils. Environmental Mechanics: Water, Mass and Energy Transport in the Biosphere: Geographical Monograph 129, Eds., P.A. Raats, O. Smiles, A.W. Warrick, American Geophysical Union 10.1029 GM13: p. 133–144.
- Libardi, P.L., Reichardt, K., Nielsen, D.R., Biggar, J.W., 1980. Simple field methods for estimating soil hydraulic conductivity. Soil Science Society of America Journal 44, 3–7.
- Mantoglou, A., Gelhar, L.W., 1987. Stochastic modeling of large-scale transient unsaturated flow system. Water Resources Research 23, 37–46.
- Polmann, D.J., McLaughlin, D., Luis, S., Gelhar, L.W., Abadou, R., 1991. Stochastic modelling of large-scale flow in heterogeneous unsaturated soils. Water Resources Research 27, 1447–1458.
- Richards, L.A., 1931. Capillary conduction of liquids in porous media. Physics 1, 318–333.

- Romano, N., 1993. Use of an inverse method and geostatistics to estimate soil hydraulic conductivity for spatial variability analysis. *Geoderma* 60, 169–186.
- Romano, N., Santini, A., 1999. Determining soil hydraulic functions from evaporation experiments by a parameter estimation approach: experimental verifications and numerical studies. *Water Resources Research* 35, 3343–3359.
- Russo, D., Bouton, M., 1992. Statistical analysis of spatial variability in unsaturated flow parameters. *Water Resources Research* 28, 1911–1925.
- Russo, D., Russo, I., Lauffer, A., 1997. On the spatial variability of parameters of the unsaturated hydraulic conductivity. *Water Resources Research* 5, 947–956.
- Wierenga, P.J., Hills, R.G., Hudson, D.B., 1991. The Las Cruces trench site: characterization, experimental results, and one dimensional flow predictions. *Water Resources Research* 27, 2695–2705.
- Yeh, T.-C.J., 1989. One-dimensional steady state infiltration in heterogeneous soils. *Water Resources Research* 25, 2149–2158.
- Yeh, T.-C.J., Harvey, D.J., 1990. Effective unsaturated hydraulic conductivity of layered sands. *Water Resources Research* 26, 1271–1279.
- Yeh, T.-C.J., Gelhar, L.W., Gutjahr, A.L., 1985a. Stochastic analysis of unsaturated flow in heterogeneous soils. 1: statistically isotropic media. *Water Resources Research* 21, 447–456.
- Yeh, T.-C.J., Gelhar, L.W., Gutjahr, A.L., 1985b. Stochastic analysis of unsaturated flow in heterogeneous soils. 2: statistically anisotropic media with variable alpha. *Water Resources Research* 21, 457–464.